Neuron, Vol. 47, 215–229, July 21, 2005, Copyright ©2005 by Elsevier Inc. DOI 10.1016/j.neuron.2005.06.026

Gliomedin Mediates Schwann Cell-Axon Interaction and the Molecular Assembly of the Nodes of Ranvier

Yael Eshed,[1] Konstantin Feinberg,[1] Sebastian Poliak,[1] Helena Sabanay,[1] Offra Sarig-Nadir,[1] Ivo Spiegel,[1] John R. Bermingham, Jr.,[2] and Elior Peles[1,*]
[1]Department of Molecular Cell Biology
The Weizmann Institute of Science
Rehovot 76100
Israel
[2]McLaughlin Research Institute
1520 23rd Street South
Great Falls, Montana 59405

Summary

Accumulation of Na^+ channels at the nodes of Ranvier is a prerequisite for saltatory conduction. In peripheral nerves, clustering of these channels along the axolemma is regulated by myelinating Schwann cells through a yet unknown mechanism. We report the identification of gliomedin, a glial ligand for neurofascin and NrCAM, two axonal immunoglobulin cell adhesion molecules that are associated with Na^+ channels at the nodes of Ranvier. Gliomedin is expressed by myelinating Schwann cells and accumulates at the edges of each myelin segment during development, where it aligns with the forming nodes. Eliminating the expression of gliomedin by RNAi, or the addition of a soluble extracellular domain of neurofascin to myelinating cultures, which caused the redistribution of gliomedin along the internodes, abolished node formation. Furthermore, a soluble gliomedin induced nodal-like clusters of Na^+ channels in the absence of Schwann cells. We propose that gliomedin provides a glial cue for the formation of peripheral nodes of Ranvier.

Introduction

Saltatory conduction along myelinated axons depends on the accumulation of voltage-gated Na^+ channels at short, regularly spaced interruptions in the myelin sheath known as the nodes of Ranvier (Waxman and Ritchie, 1993). At the nodes, these channels are found in a multiprotein complex that includes cell adhesion molecules and cytoplasmic adaptor proteins (Poliak and Peles, 2003; Salzer, 2003). Na^+ channels are associated with NrCAM and the 186 kDa isoform of neurofascin (NF186) (McEwen and Isom, 2004; Ratcliffe et al., 2001), two IgCAMs that are concentrated at the nodal axolemma (Davis et al., 1996). The interaction between these IgCAMs and Na^+ channels occurs directly (McEwen and Isom, 2004; Ratcliffe et al., 2001) or through ankyrin G (Garver et al., 1997; Lemaillet et al., 2003; Malhotra et al., 2000), an adaptor that links integral membrane proteins to the cortical cytoskeleton and is enriched at the nodes (Kordeli et al., 1990; Mohler et al., 2002). Ankyrin G binds βIV spectrin, further anchoring the nodal Na^+ channel and IgCAMs to the axonal cytoskeleton (Berghs et al., 2000; Komada and Soriano, 2002).

The position of the nodes is tightly regulated by the overlying glial cells and is not intrinsically specified by the axon (Poliak and Peles, 2003; Salzer, 2003). During the development of peripheral myelinated nerves, Na^+ channels cluster at sites adjacent to the edges of processes extended by myelinating Schwann cells (Vabnick et al., 1996), indicating that these Na^+ clusters are positioned by a direct glial cell contact. This conclusion is also supported by freeze-fracture analysis, demonstrating that the nodal specialization is always associated with Schwann cell processes (Tao-Cheng and Rosenbluth, 1983). In agreement, Na^+ channel clusters are absent after ablation of Schwann cells (Vabnick et al., 1997); they are dispersed during acute demyelination (Arroyo et al., 2004; Craner et al., 2003; Dugandzija-Novakovic et al., 1995), and reappear during remyelination (Dugandzija-Novakovic et al., 1995). In contrast to the defined requirement for direct axon-glia contact for node formation in the PNS, Na^+ clustering in the CNS might be induced by soluble factors secreted by oligodendrocytes (Kaplan et al., 2001; Kaplan et al., 1997). Whereas CNS nodes are contacted by processes of perinodal astrocytes and NG2-positive cells (Black and Waxman, 1988; Raine, 1984), PNS nodes are abutted by Schwann cell microvilli that emanate from the outer collar of the cell (Ichimura and Ellisman, 1991; Raine, 1982). These microvilli appear relatively late during the maturation of the myelin unit and develop from an early glial process that contacts the nodal axolemma (Berthold and Rydmark, 1983; Tao-Cheng and Rosenbluth, 1983). Schwann cell microvilli contain ERM proteins (ezrin, radixin, and moesin) (Melendez-Vasquez et al., 2001; Scherer et al., 2001), the ezrin binding protein EBP50 (Gatto et al., 2003), and Rho-A GTPase (Melendez-Vasquez et al., 2004), as well as syndecans (Goutebroze et al., 2003) and dystroglycan (Saito et al., 2003). ERM-positive processes have been shown to align with the developing nodes and thus were suggested to mediate axon-glia interactions necessary for the clustering of Na^+ channels (Melendez-Vasquez et al., 2001). Disruption of Schwann cell microvilli resulted in a striking reduction in nodal Na^+ channel clustering (Saito et al., 2003).

Previous studies suggested that, during the development of peripheral nodes, Na^+ channels are recruited to clusters of IgCAMs and ankyrin G that were first positioned by glial processes (Lambert et al., 1997). Addition of a soluble NrCAM (Lustig et al., 2001) or neurofascin (Koticha et al., 2005) to myelinating dorsal root ganglia cultures inhibits Na^+ channel clustering. In vivo, the appearance of Na^+ channels and ankyrin G at the nodes is delayed in *NrCAM* null mice (Custer et al., 2003), further indicating a role for the nodal IgCAMs in node formation. Here we report the identification of gliomedin, a Schwann cell ligand for both neurofascin and NrCAM that is localized to the nodal microvilli from

*Correspondence: peles@weizmann.ac.il

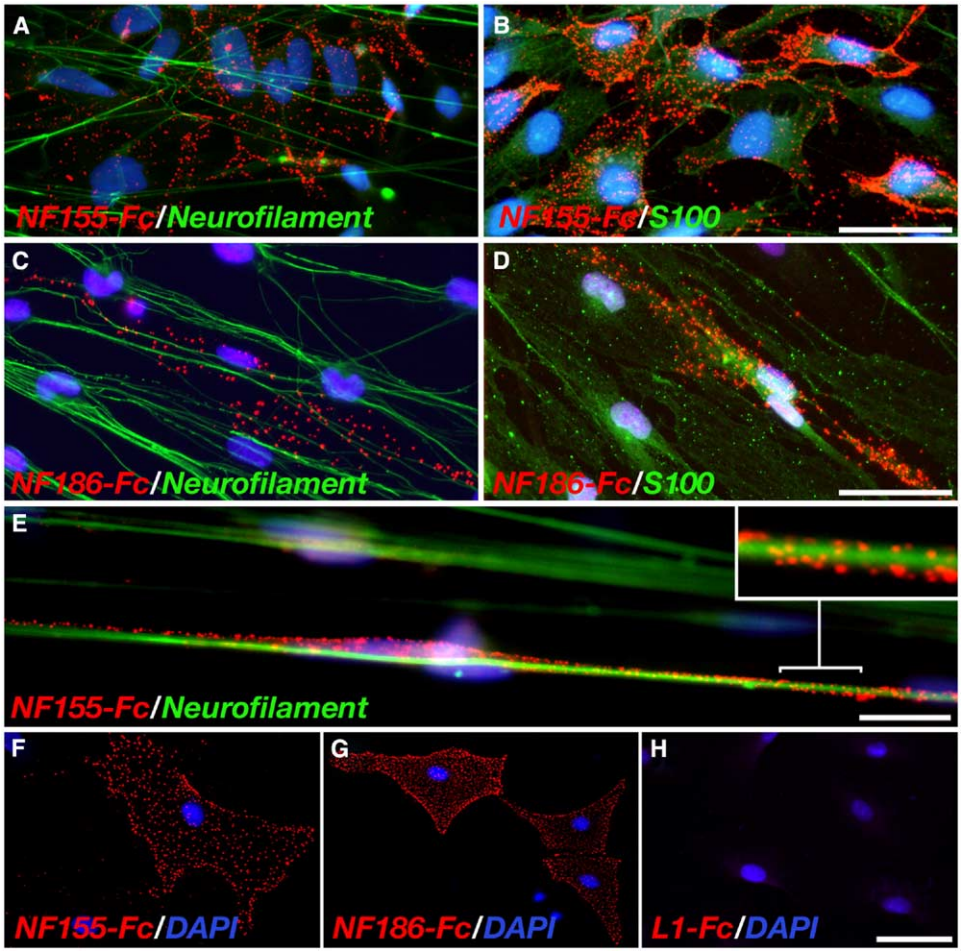

Figure 1. Soluble Neurofascin Binds Schwann Cells but Not Neurons

(A–D) Binding of NF186-Fc and NF155-Fc to DRG explants (in red). Cells were also labeled with antibodies to neurofilament to detect neurons ([A and C], in green) or S100 to detect Schwann cells ([B and D], in green) as indicated. Cell nuclei were labeled with DAPI ([A–H], in blue).

(E) Binding of NF155-Fc to a Schwann cell that is aligned with a neurofilament-labeled axon. An enlarged image of the cell process spiraling around the axon is shown in the inset.

(F–H) Binding of NF155-Fc (F), NF186-Fc (G), or L1-Fc (H) to isolated rat Schwann cells. Both neurofascin isoforms bound to most, but not all, Schwann cells in the culture.

Scale bars: 50 μm (A–D), 20 μm (E), 50 μm (F–H).

the onset of myelination. Our results suggest that Schwann cell-axon interactions mediated by gliomedin trigger the molecular assembly of the nodes of Ranvier in the PNS.

Results

Schwann Cells Exhibit Specific Binding Sites for Neurofascin

The presence of neurofascin at the nodal axolemma suggests that it may interact with a glial receptor found at the adjacent Schwann cell membrane (Lambert et al., 1997). To test this possibility, we used the extracellular domain of either the 186 kDa or 155 kDa isoforms of neurofascin fused to human Fc (NF155-Fc, NF186-Fc) in binding experiments on mixed dorsal root ganglia (DRG) cultures. Both neurofascin isoforms bound exclusively to S100-positive Schwann cells and not to neurofilament-labeled axons (Figures 1A–1D). Neurofascin binding was occasionally detected on Schwann cells at the initial stage of axon enwrapping (Figure 1E). Similarly, NF155-Fc and NF186-Fc also bound to primary cultured rat Schwann cells (Figures 1F and 1G). In contrast, Schwann cells did not bind the extracellular domain of several related IgCAMs, such as L1 (Figure 1H) or contactin (data not shown). These results suggest that Schwann cells express a specific ligand for neurofascin.

Identification of a Schwann Cell Ligand for Neurofascin

A rat Schwann cell cDNA library was constructed and screened by expression cloning in order to isolate the putative glial ligand for neurofascin. Plasmid pools made from this cDNA library were transfected into COS7 cells, which were subsequently screened for their ability to bind NF-Fc, as previously described (Peles et al.,

1995). One of six positive pools was further subdivided into smaller pools and rescreened until a single plasmid was isolated (Figure 2A). Sequence analysis of this cDNA clone revealed a single open reading frame of 1647 nucleotides, which encodes for a 549 amino acid protein (Figure 2B). The predicted polypeptide has the hallmarks of a type II transmembrane protein, containing a short (15 aa) cytoplasmic tail at its amino terminus and a carboxy-terminal extracellular region, which includes collagen triple helix repeats (COL) and a single olfactomedin domain (OLF; Figures 2B and 2C). This protein, which we termed "gliomedin," belongs to a growing family of olfactomedin-related molecules (Barembaum et al., 2000; Loria et al., 2004; Tsuda et al., 2002). A sequence corresponding to the extracellular domain of mouse gliomedin was also identified as a liver cancer-related gene (CRG-L2; Graveel et al., 2003). The presence of both OLF and COL domains in the extracellular region of gliomedin places it within a distinct subgroup of the olfactomedin proteins, recently termed "colmedins" (Loria et al., 2004). As expected, double labeling of cultured Schwann cells with NF-Fc and an antibody to gliomedin demonstrated that the extracellular domain of neurofascin only bound to cells expressing gliomedin (Figure 2D). Furthermore, all the primary positive cDNA pools originating from the screen were found to contain gliomedin, indicating that we have isolated the main Schwann cell ligand for neurofascin (data not shown).

As demonstrated by Northern blot analysis, a single 5 kb gliomedin transcript was detected in human spinal cord, brain, placenta, and sciatic nerve, but not in other tissues (see Figure S1 in the Supplemental Data available online). Direct comparison between the sciatic nerve and the brain showed that the gliomedin transcript is much more abundant in the PNS than in the CNS (Figure S1B). In situ hybridization of rat sciatic nerve demonstrated a dramatic increase in the expression of gliomedin in myelinating Schwann cells during the first postnatal week, which corresponds to the initial period of active myelination in the PNS (Figure S1C).

Gliomedin Interacts with Both Neurofascin and NrCAM

To characterize the interaction between gliomedin and cell adhesion molecules, we tested whether soluble Fc-fusion proteins containing the extracellular domain of various IgCAMs bind to cells expressing gliomedin. As depicted in Figure 2E, soluble neurofascin (both isoforms) and NrCAM specifically bound to gliomedin-expressing COS7 cells. In contrast, no binding was detected when using Fc-fusion proteins containing the extracellular domain of other IgCAMs, such as L1 and contactin. Similar binding specificity was observed using isolated Schwann cells or when a soluble gliomedin was used in binding experiments to COS7 cells expressing the different IgCAMs (data not shown). Domain mapping analysis using soluble Fc-fusion proteins containing either the extracellular domain of gliomedin (ECD-Fc), its collagen repeat (COL-Fc), or the olfactomedin domain (OLF-Fc) demonstrated that the latter mediates its interaction with neurofascin and NrCAM (Figures 2F and 2G and data not shown). When ECD-Fc was used in binding experiments on frozen sections of sciatic nerves, it specifically labeled the nodes of Ranvier, where both neurofascin and NrCAM are located (Figure 2H). Altogether, these experiments demonstrate that gliomedin binds specifically to the two IgCAMs that are found at the nodal axolemma.

Gliomedin Is a Novel Component of PNS Nodes of Ranvier

The localization of gliomedin in myelinated nerves was determined using polyclonal and monoclonal antibodies to this protein in combination with antibodies to various axonal or glial markers (Figure 3). In sciatic nerve fibers from adult rats, gliomedin antibodies labeled short (1–2 μm long) segments along the axon (Figure 3A). Double labeling using antibodies to gliomedin and MAG (a marker for non-compact myelin) revealed that gliomedin was localized at the node of Ranvier, as identified by the flanking paranodal loops stained for MAG (Figure 3B). Similarly, double immunolabeling with antibodies to gliomedin and Caspr, which marks the axoglial paranodal junction (Einheber et al., 1997), or an antibody that recognizes both isoforms of neurofascin and thus labels both nodes and paranodes (Schafer et al., 2004) demonstrated that gliomedin is found only in the nodes of Ranvier and not at the paranodes (Figures 3C–3E). The absence of gliomedin from the paranodal junction indicates that, in adult peripheral nerves, it is likely to interact with the 186 kDa isoforms of neurofascin that is found at the nodes rather than with the paranodal 155 kDa isoform (Tait et al., 2000). At the nodes, gliomedin was localized with known nodal proteins, including Na^+ channels, ankyrin G, NrCAM, and NF186 (Figures 3F–3J). Occasionally, gliomedin staining extended beyond the nodal axolemma (Figure 3I), indicating that it may be expressed in the Schwann cell microvilli, which fill the nodal gap and contact the nodal axolemma in the PNS. In contrast, gliomedin was not detected at the nodes of Ranvier in the CNS (Figures 3K–3M).

At PNS nodes, gliomedin was localized with ERM proteins (ezrin, radixin, moesin) and claudin-2, all of which are concentrated in the Schwann cell microvilli (Figure 4A) (Melendez-Vasquez et al., 2001; Poliak et al., 2002; Scherer et al., 2001). Furthermore, immunoelectron microscopic analysis of cross (Figures 4D and 4E) or longitudinal (Figures 4F–4H) sections of adult rat sciatic nerve demonstrated that gliomedin is found along the microvilli processes. Notably, double labeling for gliomedin and ERM proteins revealed that gliomedin was always associated with a microvillar membrane (data not shown). In summary, these results demonstrate that gliomedin is a novel glial component of the nodes of Ranvier in the PNS and suggest that it may play a role in mediating axoglial contact as well as in maintaining the position of the microvilli toward the nodal axolemma.

Developmental Expression of Gliomedin during Myelination

We next examined when gliomedin accumulates at the node of Ranvier during the development of peripheral nerves. Sections of rat sciatic nerves that had been col-

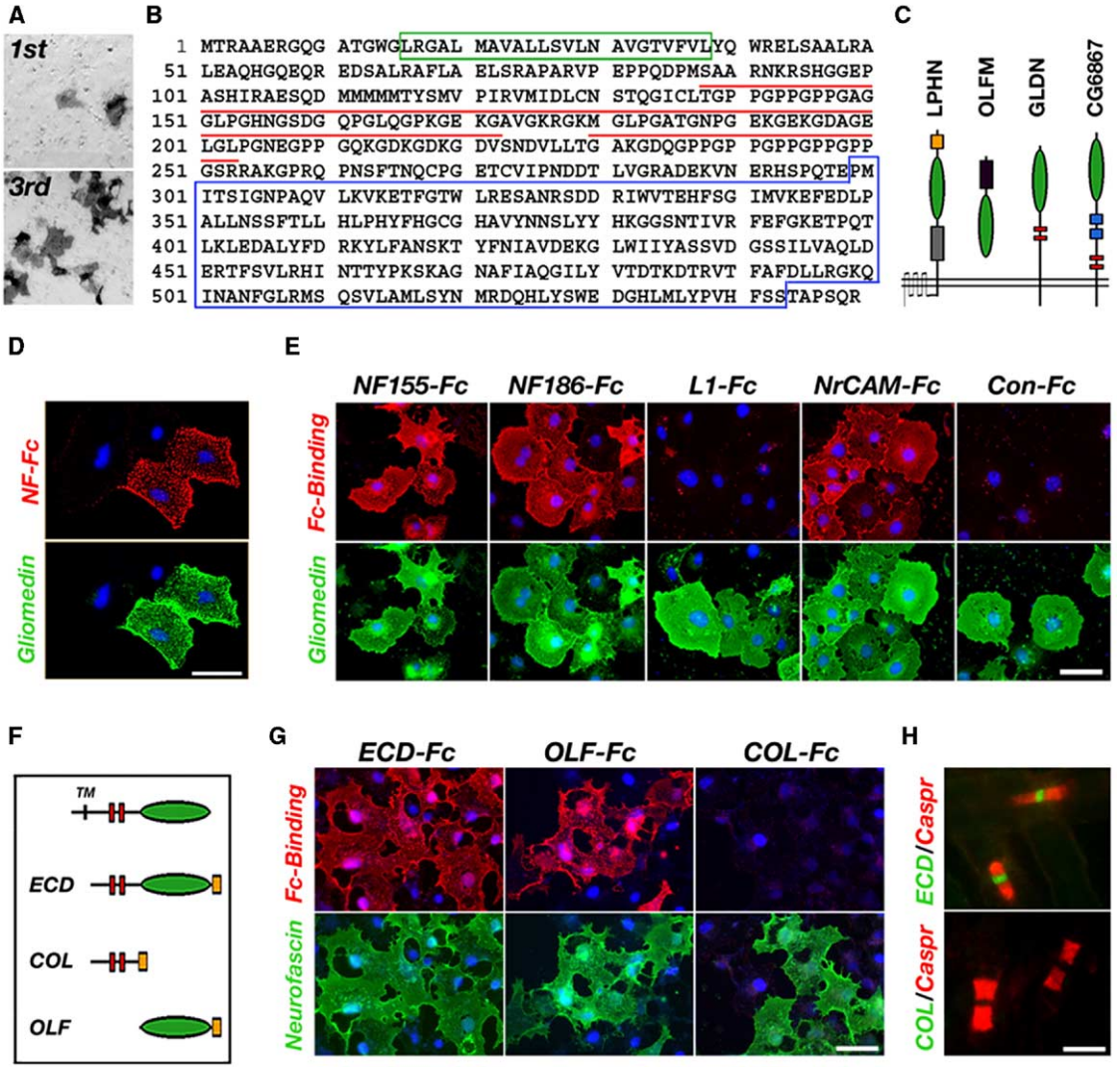

Figure 2. Identification of Gliomedin as a Glial Ligand for the Nodal IgCAMs

(A) Binding of NF-Fc to COS-7 cells transfected with one of the primary Schwann cDNA pools (1st) or a single cDNA isolated after three additional rounds of screening (3rd).

(B) The deduced amino acid sequence of rat gliomedin (NP 852047). The transmembrane domain (green box), collagen repeats (red line on top of sequence), and the olfactomedin domain (blue box) are highlighted.

(C) Domain organization of gliomedin (GLDN) compared to several representatives of the olfactomedin family. The olfactomedin domain is shown as a green ellipse and the collagen-like repeat in a red square. LPHN, latrophilin (Lelianova et al., 1997); OLFM, olfactomedin (Yokoe and Anholt, 1993); CG6867 encodes a putative transmembrane protein in *Drosophila melanogaster*. The gliomedin (GLDN) subgroup also contains UNC122 and COF-1 in *C. elegans*.

(D) Binding of neurofascin-Fc to gliomedin-expressing Schwann cells. Isolated rat Schwann cells were allowed to bind NF155-Fc (red) and then fixed and stained using an antibody to gliomedin (green) and Dapi (blue) to label nuclei. Neurofascin bound to the two gliomedin-expressing cells of the four cells present in the field.

(E) Gliomedin binds to neurofascin and NrCAM but not to other IgCAMs. Binding of different Fc-fusion proteins containing the extracellular domains of the NF155, NF186, L1, NrCAM, or contactin (Con-Fc) to COS-7 cells expressing gliomedin (upper raw; red). Expression of gliomedin on the cell surface was detected using specific antibodies (lower raw; green).

(F) Schematic presentation of the soluble gliomedin Fc-fusion proteins. ECD, extracellular domain; COL, collagen repeats; OLF, olfactomedin domain. The location of the Fc region is depicted as a yellow box.

(G) The OLF domain of gliomedin mediates its interaction with neurofascin. Binding of ECD-Fc, OLF-FC, or COL-Fc to COS-7 cells expressing neurofascin (upper row; red). The expression of neurofascin in the transfected cells was determined using specific antibodies and is shown in green in the lower panel.

(H) Binding of ECD-Fc (upper panel) and COL-Fc (Lower panel) to sections of rat sciatic nerve. The location of the paranodal junctions is labeled with antibodies to Caspr (red).

Scale bars: 10 μm (D, E, and G), 5 μm (H).

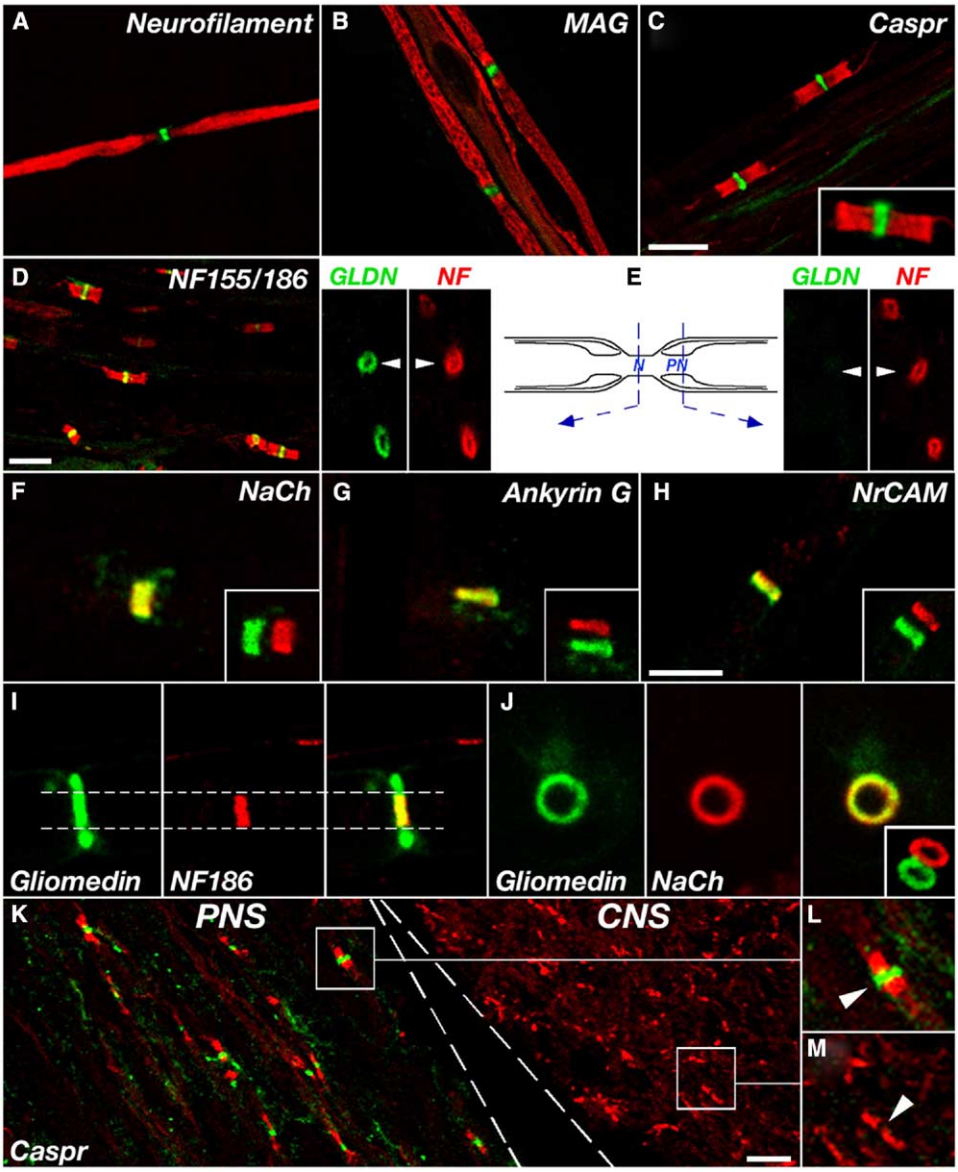

Figure 3. Gliomedin Is Localized at the Nodes of Ranvier in the PNS

(A–D) Double immunofluorescence labeling of teased adult rat sciatic nerve using an antibody to gliomedin (green in all panels) and antibodies to neurofilaments (A), MAG (B), Caspr (C), or pan-neurofascin (D), as indicated (all in red). The pan-neurofascin antibody recognizes both neurofascin isoforms, NF186 and NF155, that are found at the nodes and paranodal junction, respectively.

(E) Consecutive optical sections through the nodes and the paranodes of teased sciatic nerves labeled for gliomedin (green) and pan-neurofascin (red), along with a schematic drawing showing the location of the section. Note that while both gliomedin and neurofascin are present in the nodes, only neurofascin is found at the adjacent paranodal region.

(F–J) Higher magnification of the nodal region in teased-fiber preparations (F–I) or cross-section (J) of sciatic nerves, double-labeled with an antibody to gliomedin (green) and Na^+ channels (F and J), ankyrin G (G), NrCAM (H), or NF186 (I), as indicated (in red). Insets in panels (F)–(H) and (J) show merged images in which the green and red channels were shifted. Note that anti-gliomedin antibodies occasionally labeled the nodes outside the nodal axolemma (dotted line in panel [I]).

(K) Horizontal section of the ventral region of the spinal cord, including the ventral roots, was immunolabeled with an antibody to gliomedin (green) and Caspr (red). The border between the CNS and the PNS is depicted with a dashed line. While Caspr labeled the paranodes in both CNS and PNS, nodal labeling of gliomedin was only detected in the ventral roots and not in the spinal cord. Some weak, nonspecific staining of gliomedin is also seen outside the nodes in the PNS.

(L–M) Higher magnification of the areas marked in panel (K).

Scale bars: 10 μm (A–D), 5 μm (F–H).

lected from postnatal day 1 to 14 (P1–P14), were labeled with antibodies to gliomedin and to Na^+ channels, or to Caspr (Figure 5A). Gliomedin appeared at the node of Ranvier before Caspr accumulated at the paranodes (Figure 5A), in accordance with previous studies demonstrating that Caspr accumulated at the

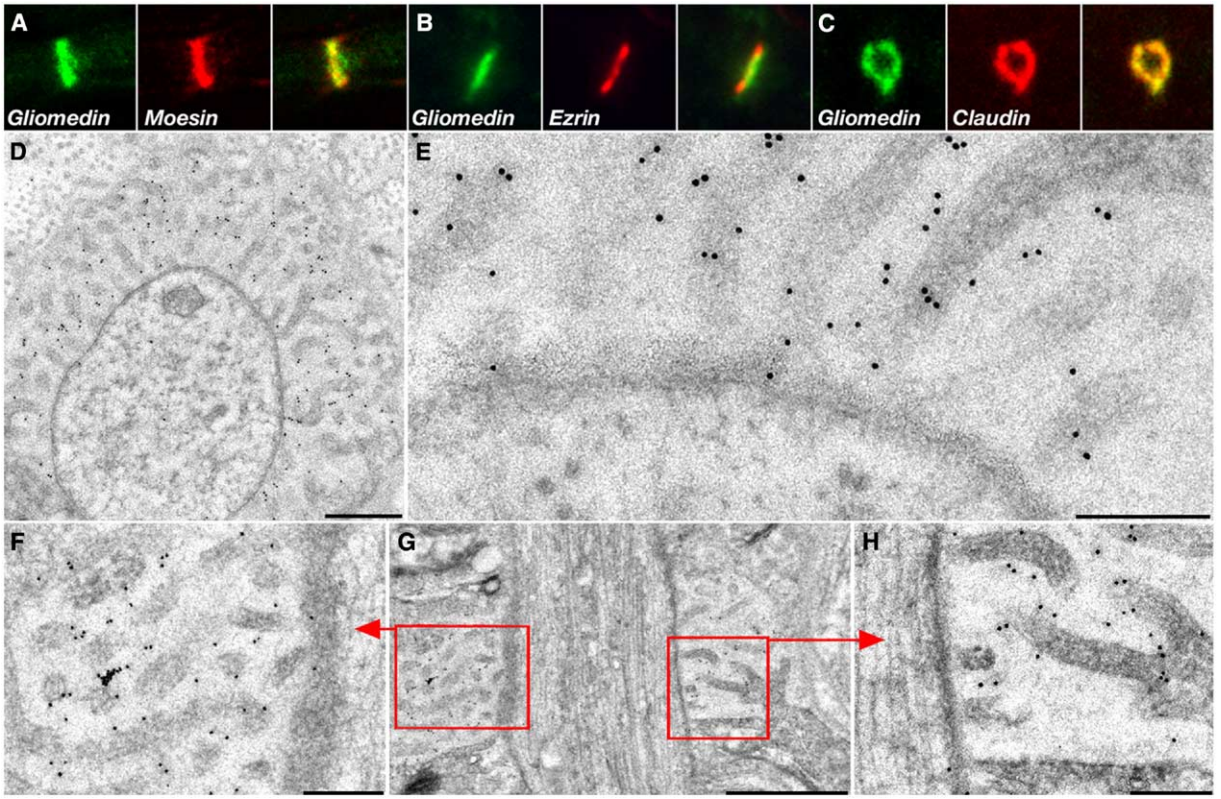

Figure 4. Gliomedin Is a Component of the Nodal Schwann Cell Microvilli

(A–C) Immunofluorescence labeling of teased sciatic nerve (A and B) or cross-section (C), using an antibody to gliomedin (in green) and antibodies to moesin (A), ezrin (B), or claudin-2 (C) as indicated (all in red).

(D–H) Immunoelectron microscopic analysis of the localization of gliomedin in adult sciatic nerve. Immunogold labeling of gliomedin on cross (D and E) or longitudinal (F–H) sections through the nodes. Note the strong labeling of the microvilli, whereas no gold particles were detected in the axon. Panels (F) and (H) show higher magnifications of the red squares labeled in (G). Note that the labeling obtained between the microvilli represents the presence of gliomedin on another microvillar membrane, which is found below the plane of the section.

Scale bars: 0.5 μm (D), 0.2 μm (E, F, and H), 1 μm (G).

paranodes shortly after ankyrin G and Na^+ channels clustered at the nodes (Melendez-Vasquez et al., 2001). Subsequently, gliomedin-labeled nodes were flanked by one or two Caspr-positive paranodes (Figures 5A and 5D). Double labeling for gliomedin and Na^+ channels demonstrated that clusters of the latter always colocalized with gliomedin (Figure 5A). As previously described for Na^+ channels (Vabnick et al., 1996; Lambert et al., 1997), in the first postnatal days, antibodies to gliomedin labeled different intermediate forms of nodal maturation, ranging from distant binary nodes to closer binary and finally to the mature focal nodes (Figure 5B). At P1, we occasionally detected gliomedin-positive sites that were negative for Na^+ channels (Figure 5C). Although it is not clear whether these early clusters indeed represent future nodes, they have been detected at the edges of MBP-labeled internodes, where Na^+ clusters usually form. In contrast, we found that gliomedin colocalized with neurofascin at all stages of development of sciatic nerve (data not shown). Triple immunolabeling of myelinating dorsal root ganglion explants with antibodies to gliomedin, MAG, and MBP demonstrated that the accumulation of gliomedin at edges of the internodes occurs with the transition between ensheathment (MAG^+/MBP^-) and the beginning of myelination (MAG^+/MBP^+) (Figure 5E). As found in developing nerves, neurofascin clusters were invariably associated with gliomedin during different stages of myelination in culture (data not shown). These results demonstrate that gliomedin accumulates at the glial membrane that contacts the early forming node.

Proper Localization of Gliomedin Is Necessary for Node Formation

To elucidate the role of gliomedin in peripheral nerves, we first examined whether the addition of a soluble Fc-fusion protein containing the extracellular domain of its receptor (i.e., NF-Fc) to myelinating cultures affected node formation. DRG explants were grown in the presence of NF-Fc, or only the Fc region as control, for 12 days after the induction of myelination as described in the Experimental Procedures. Neither Fc-fusion proteins had an affect on the ability of Schwann cells to myelinate, as determined by MBP expression (Figure 6A). However, whereas gliomedin was located at both sides of MBP-labeled segments in control cultures, in the presence of NF-Fc, it was abnormally distributed along the internodes (Figure 6A). The addition of NF-

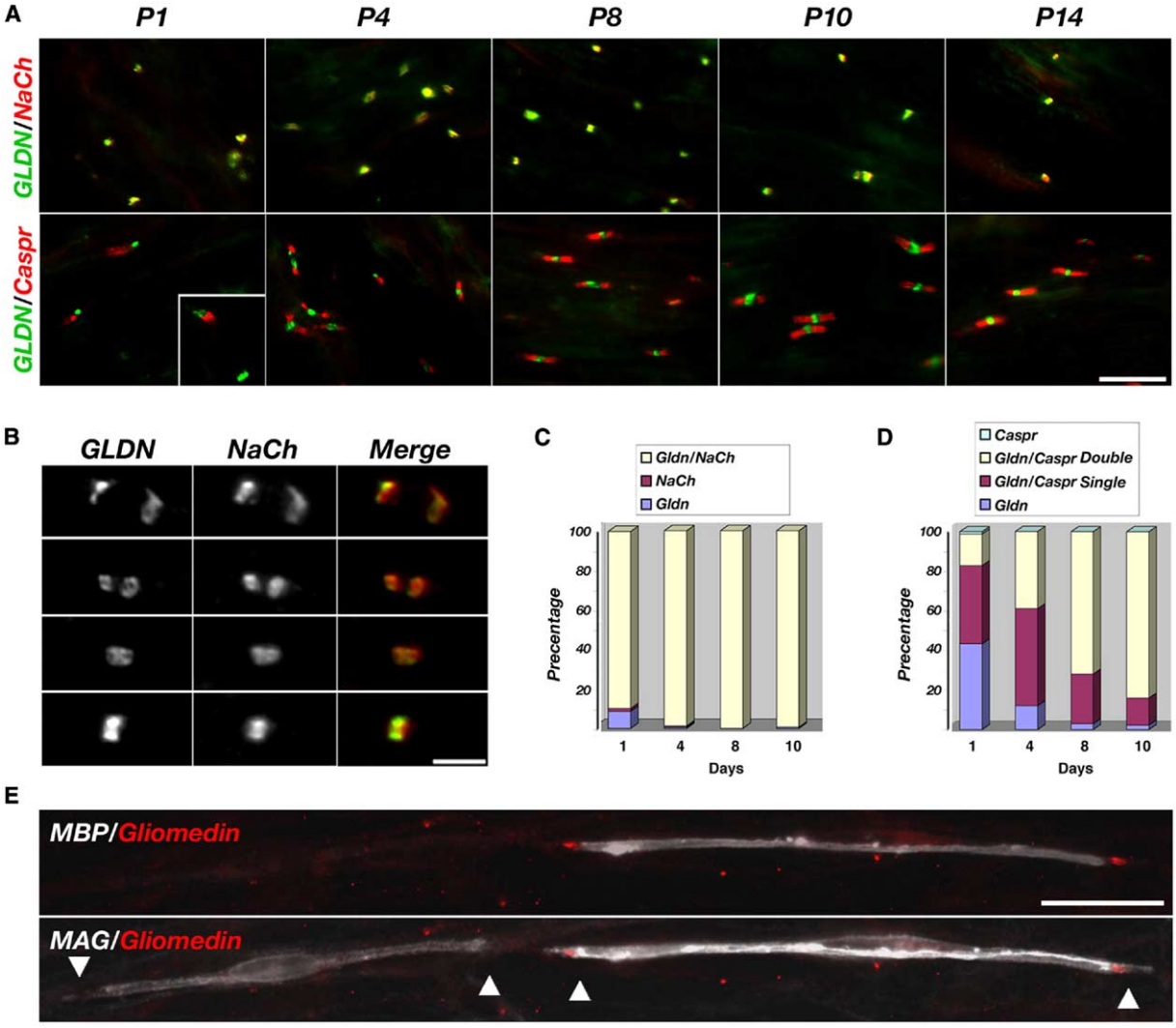

Figure 5. Gliomedin Marks the Developing Nodes

(A) Immunofluerescence labeling of longitudinal sections of 1-, 4-, 8-, 10-, and 14-day-old rat sciatic nerve with antibodies to gliomedin (green) and Na^+ channels (upper row; red) or to Caspr (lower row; red). Inset depicts another field of view.

(B) Images of developing nodes from longitudinal sections of P4 nerve double labeled with antibodies to gliomedin (left column) and Na^+ channels (middle column), as indicated. The merged images are shown on the right panel of each row. Different stages, from the immature binary form (top) to the mature focal node (bottom) are depicted.

(C) Localization of gliomedin and Na^+ channels during development. Sciatic nerve sections were labeled for gliomedin and Na^+ channels, and the number of clusters containing gliomedin (Gldn), Na^+ channels (NaCh), or both (Gldn/NaCh) were counted. The results are shown as a percentage of the total count (n = 200 sites).

(D) Developmental clustering of gliomedin compared to Caspr. Sciatic nerve sections were labeled for gliomedin and Caspr, and the numbers of sites that contained each protein alone (Caspr or Gldn) or sites containing gliomedin flanked by a single or double Caspr staining were scored (n = 200 sites).

(E) Immunolabeling of myelinating dorsal root ganglion explants 5 days after the induction of myelination with antibodies to gliomedin (red), MAG, and MBP as indicated in each panel. Clustering of gliomedin is detected in the cell on the right, which expresses both MAG and MBP, but is absent from the MAG-positive cell on the left, which has not begun to express MBP. The edges of the Schwann cells are marked with arrowheads. Scale bars: 20 μm (A and E), 5 μm (B).

Fc resulted in the clustering of gliomedin on the outer (abaxonal) membrane of the cell (Figure 6B), suggesting that binding of NF-Fc caused the displacement of gliomedin on the cell surface. This notion was further supported by the observation that similar aggregates of gliomedin were detected on the surface of Schwann cells after 2 hr incubation with NF-Fc (data not shown). The absence of gliomedin from the nodes was accompanied by a loss of axonal clustering of Na^+ channels, ankyrin G, and βIV spectrin (Figures 6A and 6C–6E). In contrast, phosphorylated ERM proteins were still present at nodal sites that lacked gliomedin (Figure 6F), indicating that treatment of NF-Fc did not disrupt Schwann cell microvilli. Furthermore, when small and

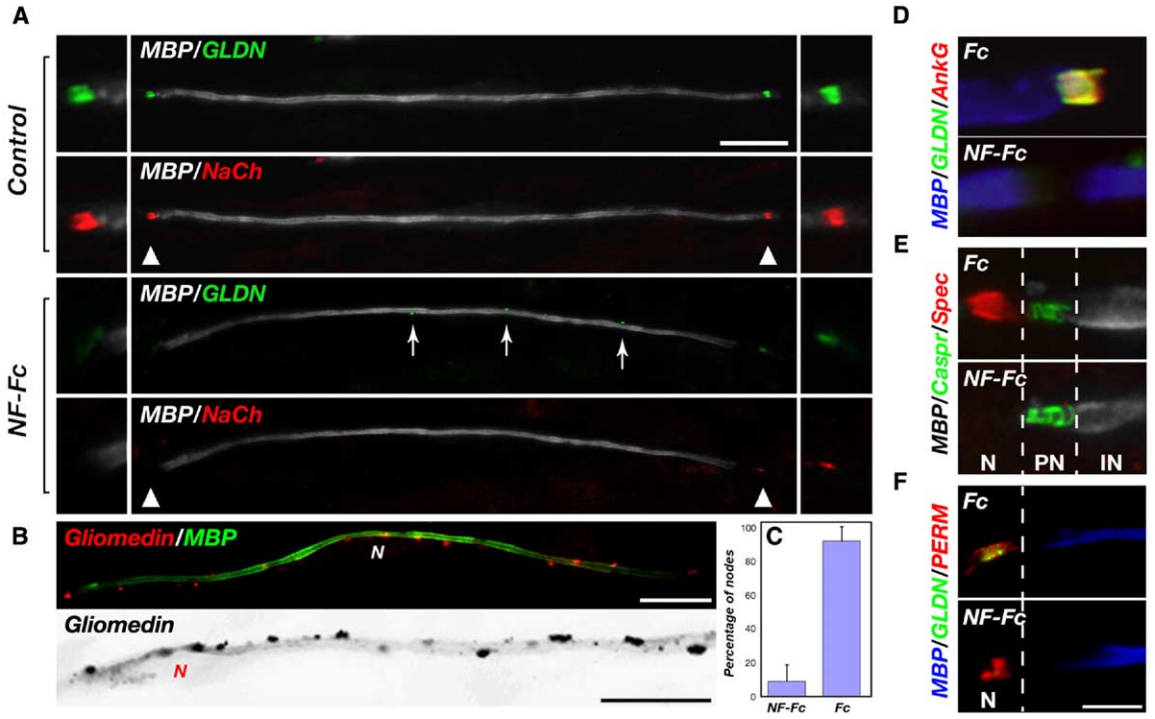

Figure 6. Treatment of Myelinating Cultures with NF-Fc Results in Redistribution of Gliomedin and Inhibition of Node Formation

(A) Immunofluorescence staining of myelinating DRG cultures that were grown in the presence of NF-Fc or a control Fc for 12 days, using antibodies to gliomedin (GLDN), Na^+ channels (NaCh), and MBP as indicated. Higher magnifications of the nodal areas (marked with arrowheads) are shown at both sides of each panel. Note that when some gliomedin was still present at the node it was associated with a small Na^+ channel cluster. Arrows in the third panel depict small clusters of gliomedin that are found along the internodes.

(B) NF-Fc causes aberrant distribution of gliomedin. (Upper panel) A myelinating Schwann cell from NF-Fc-treated culture immunolabeled with antibodies to MBP (green) and gliomedin (red). The location of the nucleus is marked (N). (Lower panel) Inverted image of another myelinating cell stained for gliomedin. Clusters of gliomedin are found on the outer (abaxonal) region of the myelin unit along the entire internodes.

(C) Quantification of MBP^+ internodes (mean ± SD) labeled for βIV spectrin and gliomedin in control (Fc) or NF-Fc-treated cultures is shown as a percentage of the total sites counted ($n = 4$; t test $p < 0.006$).

(D–F) Control (Fc) or NF-Fc-treated cultures were immunolabeled with antibodies to MBP, Caspr, gliomedin (GLDN), βIV-spectrin (Spec), ankyrin G (AnkG), or phosphorylated ERM (PERM), as indicated on the left of each panel. The position of the nodes (N), paranodes (PN), and internodes (IN) is marked with vertical lines. Scale bars: 20 μm (A), 5 μm (B).

aberrant nodal clusters of Na^+ channels were infrequently detected in the NF-Fc-treated cultures, they were always found in proximity to some residual gliomedin staining (Figure 6A, arrowhead in lower panel), demonstrating that the clustering of nodal components was invariably associated with the presence of gliomedin. Double labeling for Caspr and Na^+ channels or βIV spectrin revealed the presence of sites that lacked nodal components but were still flanked by Caspr (see for example Figure 6E), indicating that the effective nodal inhibition of NF-Fc was not secondary to paranodal abnormalities. This conclusion is further supported by previous studies demonstrating that the nodes are well formed in several paranodal mutants (Bhat et al., 2001; Boyle et al., 2001; Dupree et al., 1999; Gollan et al., 2003) and the observation that gliomedin was localized at the nodes of Ranvier in *Caspr* null mice (data not shown). In contrast to the robust effect of NF-Fc on the localization of gliomedin and node formation, we found that nodes were generated in myelinating DRG cultures treated with a soluble Fc-fusion protein containing the extracellular region of gliomedin (data not shown). This result suggests that the soluble extracellular domain of gliomedin functions as the native protein and is sufficient for initiating node formation, an idea that we tested below.

Gliomedin Is Required for Nodal Clustering of Neurofascin and Na^+ Channels

To further determine whether the expression of gliomedin in myelinating Schwann cells is essential for the clustering of nodal proteins at the axolemma, we used RNA interference (RNAi) to suppress its expression. Cultures of dissociated DRG neurons and Schwann cells were infected with retroviruses containing two different gliomedin-RNAi or a MAG-RNAi construct as control before the induction of myelination, as described in the Experimental Procedures. The infected cells were identified by the expression of GFP, which was included as a separate transcriptional unit in the viral vector used. While gliomedin clusters were present in 88% (283/322) of the MBP^+GFP^+ internodes expressing

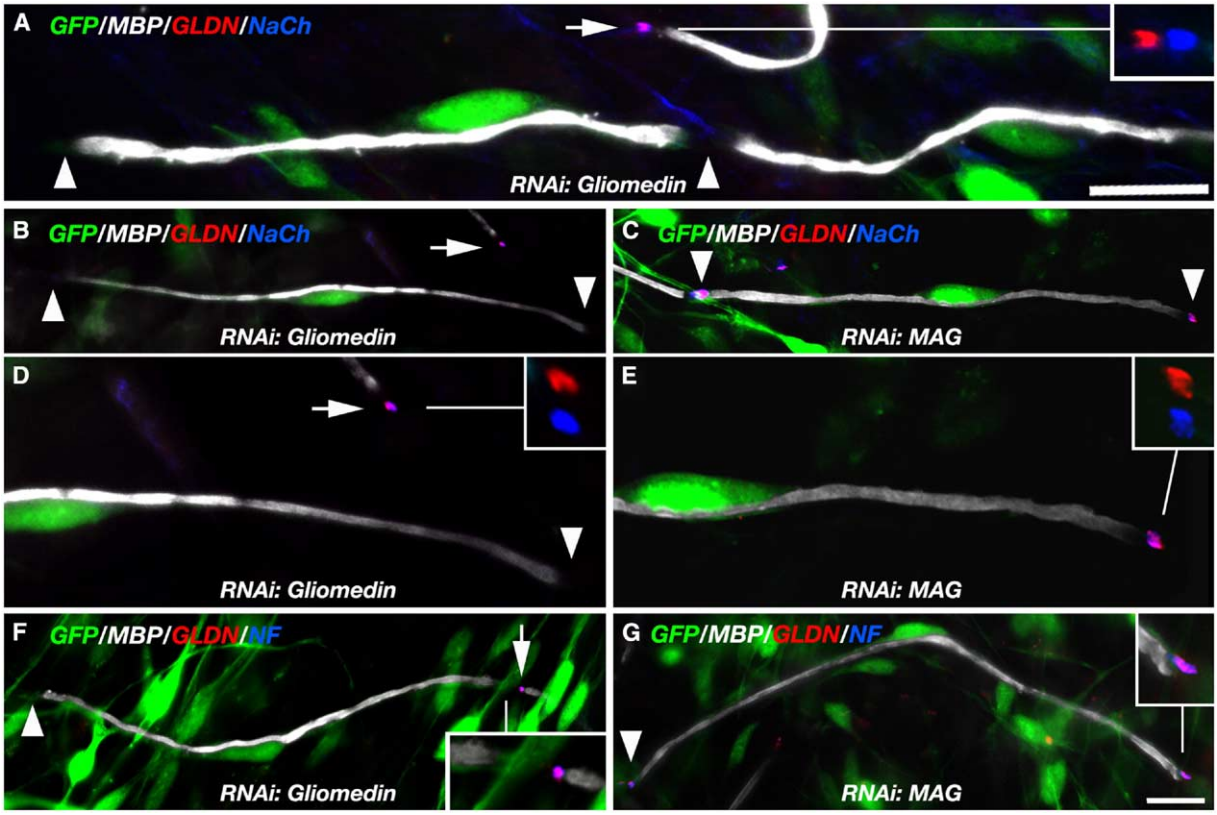

Figure 7. Gliomedin Is Required for Node Formation

DRG-derived Schwann cells were infected with retroviruses containing a GFP and RNAi designed to inhibit the expression of gliomedin (A, RNAi#1; B,D,F RNAi#3 as described in experimental procedures), or myelin associated glycoprotein (MAG; C,E,G). The cells were allowed to myelinate for 12 days and then fixed and immunolabeled with antibodies to MBP (white), gliomedin (GLDN; red) and Na^+ channels (NaCh; blue) or neurofascin (NF; blue), as indicated. The infected cells were identified by monitoring the expression of GFP (green). The right half of the internodes of the infected cell in in panels B and c are shown at a higher magnification in D and E. Arrowheads mark the location of the nodes at both sides of MBP-labeled internodes. Arrows in panels A,B,D,F depict the clustering of gliomedin and Na^+ channels or neurofascin at the edge of non-infected myelinating Schwann cells. Insets depict higher magnification of the indicated nodes; insets in A,D,E show images after shifting the red and blue channels to show the labeling of the individual components, whereas the insets in F,G show the merge images. Scale bars: 5 μm.

MAG-RNAi, they were present in only 26% (99/372) of the MBP^+GFP^+ internodes expressing gliomedin-RNAi, demonstrating the specificity of the RNAi used. Both gliomedin-RNAi and MAG-RNAi had no effect on the number of MBP-labeled internodes (Figure 7 and data not shown), indicating that neither of these genes is required for myelination, as previously demonstrated for MAG (Carenini et al., 1998). As depicted in Figure 7, suppression of gliomedin's expression by RNAi resulted in the abolishment of Na^+ channels and neurofascin clustering at the axolemma. Importantly, Na^+ channel clusters were never detected in more than 350 MBP^+GFP^+ internodes that lacked gliomedin, but were present at the edges of such internodes that still expressed it. The inhibition of node formation was specific to gliomedin-RNAi, as clusters of Na^+ channels and neurofascin were present adjacent to gliomedin at the edges of myelin internodes of noninfected cells (arrow in Figures 7A, 7B, 7D, and 7F), or cells expressing MAG-RNAi (Figures 7C, 7E, and 7G). Taken together with the inhibitory effect of NF-Fc described above, our findings demonstrate that the presence of gliomedin at the glial membrane opposing the nodes during development is necessary for the clustering of Na^+ channels at the axolemma.

Gliomedin Induces Nodal-Like Clustering in the Absence of Glial Cells

The interaction between gliomedin and the axonal IgCAMs may provide an inductive Schwann cell signal for the clustering of nodal components along the axolemma. To test this possibility, we examined whether the olfactomedin domain of gliomedin (OLF-Fc), which specifically binds neurofascin and NrCAM (Figure 2), could induce clustering of Na^+ channels in isolated DRG neurons. OLF-Fc was mixed with a Cy3-labeled antibody to human Fc and was allowed to bind purified DRG neurons for 30 min at 23°C. Further aggregation of the bound OLF-Fc by incubating the cultures at 37°C for an additional 24 hr resulted in coclustering of neurofascin (Figure 8A), underscoring its role as the axonal receptor for gliomedin. Initial clustering of neurofascin

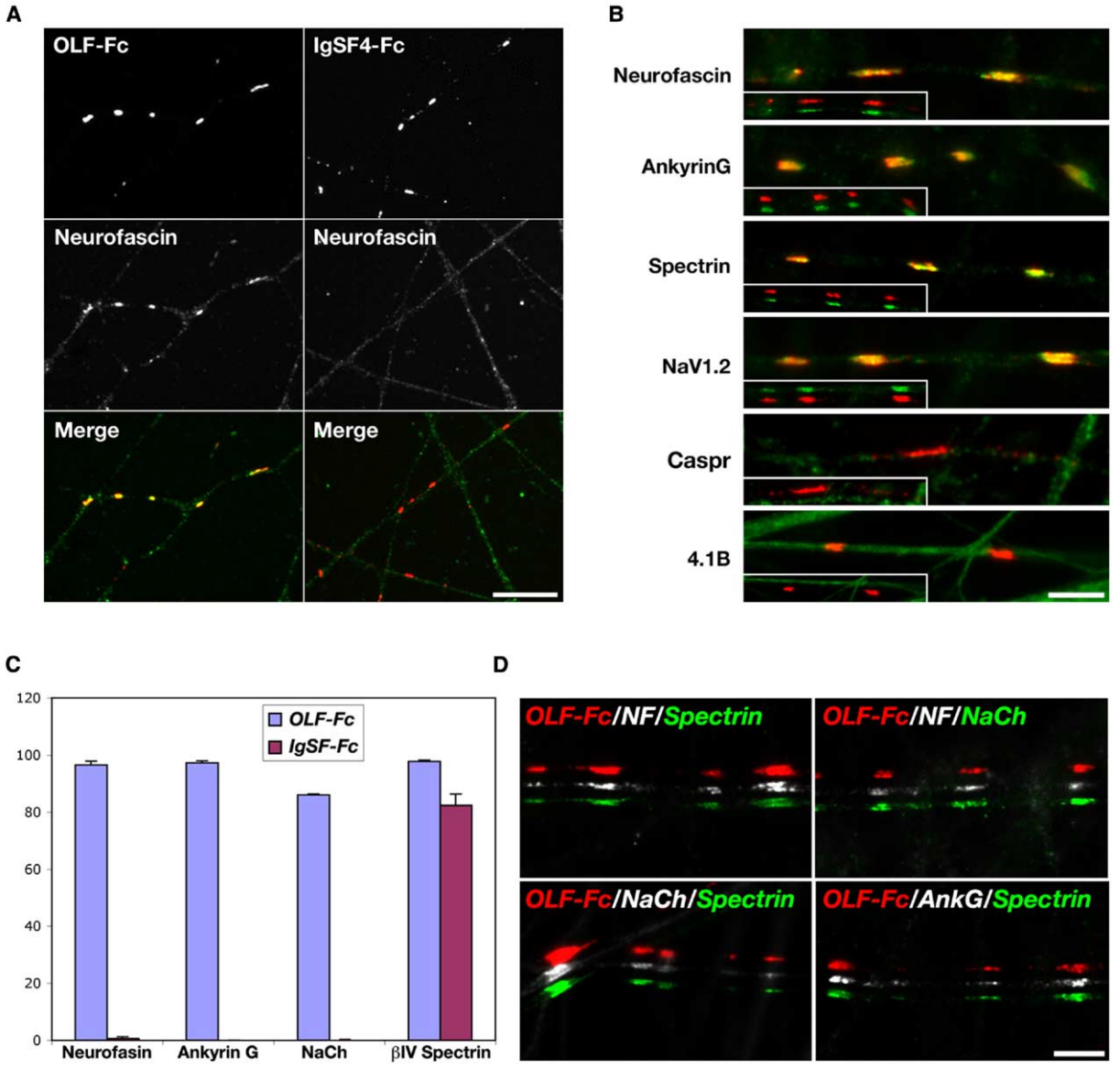

Figure 8. Soluble OLF Domain of Gliomedin Induces Nodal-Like Clusters in DRG Axons

(A) Soluble Fc-fusion proteins containing the olfactomedin domain of gliomedin (OLF-Fc) or the extracellular domain of IgSF4 (IgSF4-Fc) as control were mixed with Cy3-conjugated secondary antibody to human Fc and allowed to bind to cultures of DRG neurons. After a 30 min binding at 23°C, unbound proteins were washed away and the cultures were incubated for additional 24 hr at 37°C in growth medium before fixing. Binding of the indicated Fc-fusion proteins is shown in the upper panels, along with immunofluorescence labeling for neurofascin (middle panels) and the merge images (lower panels). (B) OLF-Fc treated DRG neurons were incubated for 48 hr at 37°C in growth medium and then fixed and immunolabeled for the bound OLF-Fc (red) and with the indicated antibodies (green). The merged images are shown for each antibody, along with images in which the green and red channels were shifted in the insets. Aggregation of gliomedin induced the clustering of all the nodal components examined but not of Caspr or protein 4.1B. Scale bars: 5 μm. (C) The number of Na^+ channels, neurofascin, ankyrin G or βIV spectrin clusters that were found adjacent to clusters of OLF-Fc or IgSF4-Fc are shown as a percentage of the total Fc clusters counted. All values are mean ± SD (n = 3). Note that while IgSF4-Fc induced the clustering of βIV spectrin, it had no effect on other nodal components including, Na^+ channels, ankyrin G and neurofascin. (D) Gliomedin-induced clusters contained several nodal proteins. DRG neurons were treated with OLF-Fc for 48 hr and then fixed and immunolabeled using a combination of antibodies as indicated in each panel. Note the co-clustering of neurofascin and spectrin, neurofascin and Na^+ channels, Na^+ channels and spectrin, as well as ankyrin G and spectrin at sites of gliomedin binding. Scale bars, 5 μm.

was already detected after incubation of the cultures for 6 hr, but was more pronounced 24–48 hr after the binding of OLF-Fc. In contrast, clustering of neurofascin was not detected using the extracellular domain of IgSF4C, an IgCAM that binds neurons (Figure 8A). Remarkably, aggregation of OLF-FC resulted in the recruitment of ankyrin G, βIV spectrin, and Na^+ channels to the neurofascin clusters (Figure 8B). In contrast to the formation of these nodal-like clusters, OLF-Fc did not induce the clustering of other none-nodal axonal

components, including transmembrane (Caspr) or cytoskeletal (protein 4.1B) proteins (Figure 8B). IgSF4-Fc, which binds an unidentified neuronal receptor distinct from neurofascin or NrCAM (I.S. and E.P., unpublished data), induced the clustering of βIV spectrin, but not of Na^+ channels, ankyrin G, or neurofascin (Figure 8C), suggesting that although βIV spectrin is required for node formation (Komada and Soriano, 2002; Lacas-Gervais et al., 2004; Parkinson et al., 2001; Yang et al., 2004), its clustering at the axonal membrane is not sufficient to induce the molecular assembly of the nodes. Quantification of these experiments revealed that 96% of the OLF-Fc clusters colocalized with neurofascin clusters, 97% with ankyrin G clusters, 86% contained Na^+ channels clusters, and 98% of these sites colocalized with βIV spectrin clusters, indicating that all of the known nodal components examined were clustered by OLF-Fc (Figure 8C). This conclusion was further supported by triple-labeling experiments demonstrating the coclustering of neurofascin with βIV spectrin or Na^+ channels, as well as of βIV spectrin with Na^+ channels or ankyrin G at sites of OLF-Fc binding (Figure 8D). Interestingly, when used without a secondary antibody, OLF-Fc bound to DRG neurons, but did not induce the formation of nodal-like clusters (data not shown). These results demonstrate that the focal accumulation of gliomedin on the axonal surface is sufficient to induce the clustering of nodal components along the axon.

Discussion

In the present study, we describe the identification of gliomedin as a glial ligand for neurofascin and NrCAM, two axonal IgCAMs that are present at the nodes of Ranvier and thought to define the initial site for subsequent assembly of Na^+ channel clusters (Lambert et al., 1997). Several lines of evidence suggest that Schwann cell-axon interactions mediated by gliomedin and the IgCAMs play a role in the assembly of the nodes of Ranvier in the PNS. (1) Gliomedin is localized at the Schwann cell microvilli that contact the nodes of Ranvier. (2) It is accumulated at the edges of myelinating Schwann cells at the time the nodes are beginning to form. (3) During development, as well as in the mature nerve, axonal clusters containing neurofascin, Na^+ channels, ankyrin G, and βIV spectrin are invariably associated with glial clustering of gliomedin. (4) Interference of the accumulation of gliomedin at the edges of Schwann cells during myelination in vitro was accompanied by a substantial reduction in Na^+ channel clustering. (5) Elimination of gliomedin's expression in myelinating Schwann cells by RNAi abolished node formation. (6) A soluble olfactomedin domain of gliomedin, which binds to the IgCAMs, was sufficient to induce nodal-like clusters along the axons of isolated DRG neurons. Taken together, our findings suggest that gliomedin acts as a local glial cue, which triggers the assembly of the nodes of Ranvier in the PNS.

Gliomedin, an Olfactomedin Domain Ligand for IgCAMs

The extracellular region of gliomedin contains olfactomedin and collagen-like domains, both of which are found in a variety of secreted and transmembrane proteins involved in cell adhesion and extracellular matrix interactions (Hillier and Vacquier, 2003; Loria et al., 2004; Yokoe and Anholt, 1993; Myllyharju and Kivirikko, 2004). Proteins containing OLF domains have been shown to play important roles in the nervous system, yet no specific receptors for these proteins have been identified. For example, UNC122, the *C. elegans* homolog of gliomedin, is expressed in muscles and has been suggested to function as an adhesion molecule at the neuromuscular synapse (Loria et al., 2004). Noelin and tiarin, two secreted OLF proteins, have been shown to be involved in neurogenesis of the neural crest and dorsal patterning of the neural tube, respectively (Barembaum et al., 2000; Tsuda et al., 2002). Myocilin/TIGR, another OLF domain-containing protein, is expressed in photoreceptor and trabecular meshwork cells in the eye and is often mutated in progressive open angle glaucoma, a neurodegenerative disease that is characterized by a continuous loss of optic nerve axons (Stone et al., 1997). Myocilin is also found in the basal/abaxonal region of the myelin sheath in the PNS, where it could participate in linking the cell to the surrounding basal lamina and the stabilization of the myelin unit (Ohlmann et al., 2003). We have shown that the OLF domain of gliomedin interacts specifically with neurofascin and NrCAM, but not with several related IgCAMs. This finding provides evidence that an OLF domain-containing protein interacts with members of the IgCAM superfamily, which mediates various cell adhesion and recognition events during the development and maintenance of the nervous system. Interestingly, the binding of NrCAM but not of neurofascin, to gliomedin-expressing cells required preclustering with a secondary antibody (data not shown), indicating that these two IgCAMs display different avidities toward gliomedin. This observation may explain the previously reported lack of NrCAM-Fc binding to Schwann cells (Lustig et al., 2001). At present, it is not clear whether gliomedin interacts with both IgCAMs simultaneously, or with each one separately in vivo.

Gliomedin Is a Novel Glial Component of PNS Nodes

By using in situ hybridization we found that gliomedin is expressed in myelinating Schwann cells from the onset of myelination. The expression of gliomedin in sciatic nerve starts at P1 and increases thereafter, suggesting that it is a myelin-related gene. Its expression in Schwann cells is downregulated in the absence of Oct-6 (Bermingham et al., 2002) or Krox-20 (data not shown), both of which control the expression of myelin-specific genes. Immunofluorescence and immunoelectron microscopic analysis demonstrated that, in the adult peripheral nerves, gliomedin is localized at the nodes of Ranvier, where it is present along the Schwann cell microvilli that fill the nodal gap and contact the axon. Although not much is known about the assembly of Schwann cell microvilli, they are thought to develop from an early cell process that contacts the future nodal axolemma (Berthold and Rydmark, 1983; Tao-Cheng and Rosenbluth, 1983). The observation that gliomedin is not solely concentrated at the axonal interface of the

microvilli suggests that, in addition to mediating axon-glia interactions during development, it may play a role in maintaining the position of the microvilli toward the nodal axolemma in the mature nerve. This notion is further supported by the ability of several OLF-containing proteins to create higher-ordered oligomers (Yokoe and Anholt, 1993), as well as by the presence of a collagen-like domain in the extracellular domain of gliomedin. Collagen domains are found in many extracellular matrix proteins that play an important role in maintaining the structural organization of various tissues (Myllyharju and Kivirikko, 2004). Indeed, we found that, while the OLF domain of gliomedin binds to neurons, its COL domain binds to Schwann cells (data not shown). Future studies should determine whether, in addition to its ability to bind IgCAMs as reported here, gliomedin also interacts with other proteins that are located at the microvilli, such as syndecans and dystroglycan (Goutebroze et al., 2003; Saito et al., 2003). The possibility that gliomedin interacts with dystroglycan is of particular interest, as the latter contains an Ig-like domain in its extracellular domain, and its ablation in myelinating Schwann cells resulted in the disruption of the microvilli and substantial reduction in the clustering of Na^+ channels (Saito et al., 2003).

Role of Gliomedin in the Formation of Peripheral Nodes of Ranvier

During development of myelinated axons in the PNS, Na^+ channels initially cluster at heminodes that are associated with myelinating Schwann cells (Vabnick et al., 1996). These initial clusters, located at the edge of two neighboring cells, appear to move toward each other until they fuse and form the condensed cluster found in the mature node. Developmental analysis of the sciatic nerves showed that Na^+ channels and neurofascin clusters were invariably associated with glial clusters of gliomedin in all intermediate forms of nodal maturation. At P1, we detected few gliomedin clusters that lacked Na^+ channels, suggesting that gliomedin accumulates at the nodes just prior to the arrival of Na^+ channels. The accumulation of gliomedin at these prenodal sites resembles that of neurofascin and NrCAM, both of which were shown to be clustered before sodium channels in the PNS (Custer et al., 2003; Lambert et al., 1997). Analysis of myelinating DRG cultures revealed that gliomedin accumulated at the edge of MAG-labeled Schwann cells once they have started to express MBP. Na^+ channel clusters always colocalized with clusters of gliomedin, indicating that nodal clustering occurs only in association with ensheathing Schwann cells that have already begun to myelinate. Thus, early on during myelination, gliomedin accumulates at the glial cell processes that contact the axon, where it is properly positioned in order to mediate axon-glia interactions during node formation.

We demonstrated that binding and aggregation of a soluble olfactomedin domain of gliomedin on the surface of isolated DRG neurons induces the formation of nodal-like clusters containing neurofascin, Na^+ channels, ankyrin G, and βIV spectrin. These results have two important implications. First, they provide evidence that the clustering of the axonal IgCAMs is sufficient to trigger the molecular assembly of the nodes. Second, they indicate that, when presented focally at both ends of myelinating Schwann cells, gliomedin may act as an instructive cue for the initial clustering of the axonal IgCAMs and subsequent node formation. The latter notion is further supported by the observations that eliminating gliomedin's expression by RNAi or the addition of NF-Fc to myelinating DRG cultures, which caused an unusual accumulation of gliomedin in aggregates on the abaxonal surface of myelinating Schwann cells, were accompanied by a profound inhibition of axonal clustering of Na^+ channels, ankyrin G, βIV spectrin, and neurofascin. Whether this inhibition is also accompanied by changes in the nodal architecture will ultimately require ultrastructural analysis. Furthermore, the absence of neurofascin from sites that lacked gliomedin in these cultures strongly suggests that the initial clustering of the IgCAMs at the axolemma depends on the focal accumulation of gliomedin. These results are in agreement with recent observations describing that soluble NF155 and NF186 inhibit node formation in sensory neuron-Schwann cell cultures (Koticha et al., 2005). The role of gliomedin as an instructive Schwann cell signal is also supported by the observation that, in contrast to NF-Fc, a soluble gliomedin (ECD-Fc) did not inhibit node formation in myelinated DRG cultures. While NF-Fc binds and displaces gliomedin along the Schwann cell membrane, ECD-Fc interacts with neurofascin and NrCAM primarily on regions of the axon that are free of Schwann cells, where it can actually induce their clustering. In agreement, we found that in myelinating cultures the added ECD-Fc was associated with ectopic clusters of ankyrin G at the axonal initial segment and cell soma (data not shown).

Our results support a two-step mechanism for the formation of PNS nodes. In axons before myelination, neurofascin, NrCAM, and Na^+ channels are all distributed along the axolemma, while ankyrin G is found in the cytoplasm (Davis et al., 1996; Lambert et al., 1997). When ensheathing Schwann cells begin to myelinate, gliomedin is accumulated at the edges of Schwann cells, where it is focally presented to the axon. At these sites, binding of gliomedin to neurofascin and NrCAM causes their initial clustering into higher-ordered oligomers, which facilitates the recruitment of ankyrin G (Mohler et al., 2002). In addition, binding of gliomedin may affect the phosphorylation of these IgCAMs on a conserved tyrosine residue (FIGQY), which is known to regulate their interaction with ankyrin G, and their lateral mobility at the plasma membrane (Garver et al., 1997). In the second phase, these initial clusters enable the subsequent assembly of larger complexes containing Na^+ channels, as well as βIV spectrin, which in turn provides further linkage to the axonal cytoskeleton (Komada and Soriano, 2002; Lacas-Gervais et al., 2004; Parkinson et al., 2001; Yang et al., 2004). This resembles the mechanism operating during the molecular assembly of postsynaptic glutamatergic synapses, where aggregation of neuroligin by focal presentation of neurexin induces the clustering of PSD-95, which in turn leads to the assembly of large protein complexes (Graf et al., 2004). At present, it is not clear whether the subsequent recruitment of Na^+ channels to the site of the interaction between gliomedin and IgCAMs occurs as

a result of lateral diffusion of these channels along the axolemma (Custer et al., 2003) or by specific sorting and targeting mechanism, as has been recently shown to regulate the accumulation of Na^+ channels in the axonal initial segment (Fache et al., 2004).

In the PNS, the length of the internodes and thus the location of the nodes are intrinsically determined by myelinating Schwann cells (Court et al., 2004; Melendez-Vasquez et al., 2004). Our results suggest that axon-glia interaction mediated by gliomedin and the IgCAMs constitutes part of the mechanism by which myelinating Schwann cells dictate the location of the nodes of Ranvier along these axons. Different mechanisms may operate in the CNS, where nodal clustering requires the presence of oligodendrocytes (Mathis et al., 2001), but not of myelination (Arroyo et al., 2004). In contrast to Schwann cells (Ching et al., 1999), mature oligodendrocytes secrete a soluble factor that induces the formation of nodal-like clusters in retinal ganglion neurons (Kaplan et al., 1997, 2001). An intriguing possibility raised by our findings is that the initial clustering of these channels in the CNS by a secreted oligodendrocyte factor could result from its binding to the axonal IgCAMs. This would then imply that the mechanisms by which oligodendrocytes and myelinating Schwann cells regulate the clustering of Na^+ channels along the axolemma might not be so different after all.

Experimental Procedures

Tissue Culture Methods

Dissociated rat DRG cultures were grown in Neurobasal medium (Gibco) supplemented with B27 (Gibco) and 50 ng/ml NGF (Alomone labs) (NB medium) for 5 days before being used in binding experiments. Purified DRG neurons were established by treating dissociated mixed cultures with two cycles (2 days each) of NB medium containing 10 μM uridine/10 μM 5′-Fluoro 2′-deoxyuridine (Sigma) to eliminate fibroblasts and Schwann cells. Myelinating DRG cultures were maintained for 2 days in NB medium and then switched to Basal Eagle's medium (BME; Gibco) containing ITS supplements (Sigma), 0.2% BSA, 4 g/l D-glucose, and 50 ng/ml NGF (BN medium). Myelination was induced after an additional 10 days by the addition of 15% heat-inactivated FCS (Gibco) and 50 μg/ml L-ascorbic acid (Sigma) (BNC medium). Viral infection was carried out for 2 hr with 8 μg/ml polybrene on the second, third, and fourth days after plating with undiluted viral stock; myelination was induced 6 days later and proceeded for an additional 12 days before analysis.

Expression Cloning

Construction of the rat Schwann cell cDNA library and expression cloning was done essentially as described previously (Peles et al., 1995). One positive pool was subdivided and rescreened three additional times until a single clone (F10) was isolated. DNA sequencing of the isolated clone was performed on both strands (GenBank accession number AY266116).

Constructs and Antibodies

Fc-fusions containing the collagen repeats (COL, residues 138–253) and the olfactomedin domain (OLF, residues 299–543) were made by cloning the corresponding DNA to pSecTagA vector (Invitrogen), which contains the signal sequence of the κ chain of human IgG, and then transferred to pCX-Fc (Gollan et al., 2003). NF186Fc, L1-Fc and NrCAM-Fc (Lustig et al., 2001) were obtained from Martin Grumet. Contactin-Fc was described previously (Peles et al., 1995). RNAi constructs for rat gliomedin (target sequence RNAi #1, tgagcgccattctccacaa; target sequence RNAi #3, acaactctctc tactacca) and rat MAG (target sequence, catggcgtctggtatttca) were cloned into a modified pRETRO-SUPER vector (Brummelkamp et al., 2002) in which the puromycin resistance gene was replaced with an EGFP (Clontech). Retroviral stocks were prepared using the Helper virus-free Phoenix-Eco packaging cells (kindly provided by G. Nolan, Stanford, CA).

Polyclonal antibodies to gliomedin were generated by immunizing rabbits with synthetic peptides corresponding to amino acid residues 273–287 (CVIPNDDTLVGRA; Ab 7202) present in the extracellular region of rat gliomedin. Monoclonal MAb94 antibody to gliomedin was generated by immunizing mice with the above extracellular-containing peptide. Rabbit polyclonal and mouse monoclonal antibodies to Caspr (Peles et al., 1997; Poliak et al., 1999), chick anti-βIV spectrin (Komada and Soriano, 2002), and rabbit anti-NrCAM (Lustig et al., 2001) were previously described. Pan-neurofascin monoclonal antibody was obtained from Matthew Rasband and rabbit anti-NF186 antibody from Peter Brophy. Other primary antibodies, including rat anti-MBP (Chemicon), mouse anti-neurofilaments (Sigma), mouse anti-Na^+ channels (Sigma), mouse anti-MAG (clone 513; Roche), and mouse anti-ankyrin G (Santa Cruz) were obtained from commercial sources. Cy3, Cy5, and Alexa-conjugated secondary antibodies were purchased from Jackson laboratory and Molecular Probes, respectively.

RNA Expression Analysis

Northern blot analysis of multiple human tissues RNA samples (BD Bioscience) was performed as previously described (Spiegel et al., 2002) using a 1 kb fragment of human gliomedin cDNA. For rat tissues, a blot containing total RNA from sciatic nerve and brain was hybridized to a 964 nucleotide BglI/EcoRI DNA fragment of rat gliomedin. In situ hybridization was performed using cRNA probe containing the entire gliomedin cDNA as previously described (Spiegel et al., 2002).

Immunofluorescence and Immunoelectron Microscopy

Teased sciatic nerves and frozen sections were prepared and immunolabeled as previously described (Poliak et al., 2002, 2003). A detailed step-by-step protocol for tissue processing and immunoelectron microscopy is available upon request. Briefly, fixed tissue was embedded in 7% agar noble, sectioned on a vibrotome, infiltrated in LR Gold, and embedded in gelatine capsules, followed by UV polymerization. Tissue sections on formvar-coated nickel grids were blocked with 0.5 BSA, 0.5% gelatine from porcine skin, 0.1% Tween-20 in PBS, and incubated with affinity purified anti-gliomedin antibody in the same buffer for 2 hr in room temperature. Grids were washed seven times in PBS and incubated for 1 hr with goat anti-rabbit IgG conjugated to 10 nm gold (1:20; Aurion). Grids were postfixed in 2% aqueous OsO_4, stained with 2% uranyl acetate and Reynolds's lead citrate, and examined using a Philips CM-12 transmission electron microscope.

Fc-Fusion Binding, Clustering, and Perturbation Experiments

Binding experiments were performed using various Fc-fusion proteins that were already incubated with Cy3-conjugated anti-human Fc (Jackson Laboratories) as described previously (Gollan et al., 2003). For clustering experiments, DRG neurons were grown for 12–13 days on slides coated with 100 μg/ml Poly-D-lysine (Sigma) and 10 μg/ml laminin (Sigma) before binding. The neurons were then incubated with medium containing OLF-Fc, GLDN-Fc, or IgSF4-Fc as described above, washed once with Neurobasal medium and grown for additional 48–72 hr in NB before fixing and staining. Quantification was done from two 72 hr and one 48 hr experiment by counting the number of OLF-FC or IgSF4-Fc sites (1.5–4.5 μm) containing Na^+ channels, neurofascin, ankyrin G, or βIV spectrin. For Fc perturbation experiments, 100 mg/ml purified proteins were added to DRG explants with the induction of myelination and was replaced every second day. The cultures were fixed and stained after additional 12–15 days.

Supplemental Data

The Supplemental Data for this article can be found online at http://www.neuron.org/cgi/content/full/47/2/215/DC1/.

Acknowledgments

We would like to thank Peter Brophy, Masayuki Komada, Martin Gurmet, Reuven Agami, and Matt Rasband for their generous gift of different antibodies and plasmids; Peter Maurel and Jim Salzer for their help with the myelinating cultures; and Steve Lambert for critical comments on the manuscript. This work was supported by grants from the National Multiple Sclerosis Society (RG3594-A-4) and the NIH (NINDS grant NS50220). E.P. is Incumbent of the Madeleine Haas Russell Career Development Chair.

Received: February 15, 2005
Revised: May 16, 2005
Accepted: June 26, 2005
Published: July 20, 2005

References

Arroyo, E.J., Sirkowski, E.E., Chitale, R., and Scherer, S.S. (2004). Acute demyelination disrupts the molecular organization of peripheral nervous system nodes. J. Comp. Neurol. *479*, 424–434.

Barembaum, M., Moreno, T.A., LaBonne, C., Sechrist, J., and Bronner-Fraser, M. (2000). Noelin-1 is a secreted glycoprotein involved in generation of the neural crest. Nat. Cell Biol. *2*, 219–225.

Berghs, S., Aggujaro, D., Dirkx, R., Jr., Maksimova, E., Stabach, P., Hermel, J.M., Zhang, J.P., Philbrick, W., Slepnev, V., Ort, T., and Solimena, M. (2000). betaIV spectrin, a new spectrin localized at axon initial segments and nodes of ranvier in the central and peripheral nervous system. J. Cell Biol. *151*, 985–1002.

Bermingham, J.R., Jr., Shumas, S., Whisenhunt, T., Sirkowski, E.E., O'Connell, S., Scherer, S.S., and Rosenfeld, M.G. (2002). Identification of genes that are downregulated in the absence of the POU domain transcription factor pou3f1 (Oct-6, Tst-1, SCIP) in sciatic nerve. J. Neurosci. *22*, 10217–10231.

Berthold, C.H., and Rydmark, M. (1983). Electron microscopic serial section analysis of nodes of Ranvier in lumbosacral spinal roots of the cat: ultrastructural organization of nodal compartments in fibres of different sizes. J. Neurocytol. *12*, 475–505.

Bhat, M.A., Rios, J.C., Lu, Y., Garcia-Fresco, G.P., Ching, W., St Martin, M., Li, J., Einheber, S., Chesler, M., Rosenbluth, J., et al. (2001). Axon-glia interactions and the domain organization of myelinated axons requires neurexin IV/Caspr/Paranodin. Neuron *30*, 369–383.

Black, J.A., and Waxman, S.G. (1988). The perinodal astrocyte. Glia *1*, 169–183.

Boyle, M.E., Berglund, E.O., Murai, K.K., Weber, L., Peles, E., and Ranscht, B. (2001). Contactin orchestrates assembly of the septate-like junctions at the paranode in myelinated peripheral nerve. Neuron *30*, 385–397.

Brummelkamp, T.R., Bernards, R., and Agami, R. (2002). Stable suppression of tumorigenicity by virus-mediated RNA interference. Cancer Cell *2*, 243–247.

Carenini, S., Montag, D., Schachner, M., and Martini, R. (1998). MAG-deficient Schwann cells myelinate dorsal root ganglion neurons in culture. Glia *22*, 213–220.

Ching, W., Zanazzi, G., Levinson, S.R., and Salzer, J.L. (1999). Clustering of neuronal sodium channels requires contact with myelinating Schwann cells. J. Neurocytol. *28*, 295–301.

Court, F.A., Sherman, D.L., Pratt, T., Garry, E.M., Ribchester, R.R., Cottrell, D.F., Fleetwood-Walker, S.M., and Brophy, P.J. (2004). Restricted growth of Schwann cells lacking Cajal bands slows conduction in myelinated nerves. Nature *431*, 191–195.

Craner, M.J., Lo, A.C., Black, J.A., and Waxman, S.G. (2003). Abnormal sodium channel distribution in optic nerve axons in a model of inflammatory demyelination. Brain *126*, 1552–1561.

Custer, A.W., Kazarinova-Noyes, K., Sakurai, T., Xu, X., Simon, W., Grumet, M., and Shrager, P. (2003). The role of the ankyrin-binding protein NrCAM in node of Ranvier formation. J. Neurosci. *23*, 10032–10039.

Davis, J.Q., Lambert, S., and Bennett, V. (1996). Molecular composition of the node of Ranvier: identification of ankyrin-binding cell adhesion molecules neurofascin (mucin+/third FNIII domain-) and NrCAM at nodal axon segments. J. Cell Biol. *135*, 1355–1367.

Dugandzija-Novakovic, S., Koszowski, A.G., Levinson, S.R., and Shrager, P. (1995). Clustering of Na^+ channels and node of Ranvier formation in remyelinating axons. J. Neurosci. *15*, 492–503.

Dupree, J.L., Girault, J.A., and Popko, B. (1999). Axo-glial interactions regulate the localization of axonal paranodal proteins. J. Cell Biol. *147*, 1145–1152.

Einheber, S., Zanazzi, G., Ching, W., Scherer, S., Milner, T.A., Peles, E., and Salzer, J.L. (1997). The axonal membrane protein Caspr, a homologue of neurexin IV, is a component of the septate-like paranodal junctions that assemble during myelination. J. Cell Biol. *139*, 1495–1506.

Fache, M.P., Moussif, A., Fernandes, F., Giraud, P., Garrido, J.J., and Dargent, B. (2004). Endocytotic elimination and domain-selective tethering constitute a potential mechanism of protein segregation at the axonal initial segment. J. Cell Biol. *166*, 571–578.

Garver, T.D., Ren, Q., Tuvia, S., and Bennett, V. (1997). Tyrosine phosphorylation at a site highly conserved in the L1 family of cell adhesion molecules abolishes ankyrin binding and increases lateral mobility of neurofascin. J. Cell Biol. *137*, 703–714.

Gatto, C.L., Walker, B.J., and Lambert, S. (2003). Local ERM activation and dynamic growth cones at Schwann cell tips implicated in efficient formation of nodes of Ranvier. J. Cell Biol. *162*, 489–498.

Gollan, L., Salomon, D., Salzer, J.L., and Peles, E. (2003). Caspr regulates the processing of contactin and inhibits its binding to neurofascin. J. Cell Biol. *163*, 1213–1218.

Goutebroze, L., Carnaud, M., Denisenko, N., Boutterin, M.C., and Girault, J.A. (2003). Syndecan-3 and syndecan-4 are enriched in Schwann cell perinodal processes. BMC Neurosci. *4*, 29.

Graf, E.R., Zhang, X., Jin, S.X., Linhoff, M.W., and Craig, A.M. (2004). Neurexins Induce Differentiation of GABA and Glutamate Postsynaptic Specializations via Neuroligins. Cell *119*, 1013–1026.

Graveel, C.R., Harkins-Perry, S.R., Acevedo, L.G., and Farnham, P.J. (2003). Identification and characterization of CRG-L2, a new marker for liver tumor development. Oncogene *22*, 1730–1736.

Hillier, B.J., and Vacquier, V.D. (2003). Amassin, an olfactomedin protein, mediates the massive intercellular adhesion of sea urchin coelomocytes. J. Cell Biol. *160*, 597–604.

Ichimura, T., and Ellisman, M.H. (1991). Three-dimensional fine structure of cytoskeletal-membrane interactions at nodes of Ranvier. J. Neurocytol. *20*, 667–681.

Kaplan, M.R., Meyer-Franke, A., Lambert, S., Bennett, V., Duncan, I.D., Levinson, S.R., and Barres, B.A. (1997). Induction of sodium channel clustering by oligodendrocytes. Nature *386*, 724–728.

Kaplan, M.R., Cho, M.H., Ullian, E.M., Isom, L.L., Levinson, S.R., and Barres, B.A. (2001). Differential control of clustering of the sodium channels Na(v)1.2 and Na(v)1.6 at developing CNS nodes of Ranvier. Neuron *30*, 105–119.

Komada, M., and Soriano, P. (2002). [Beta]IV-spectrin regulates sodium channel clustering through ankyrin-G at axon initial segments and nodes of Ranvier. J. Cell Biol. *156*, 337–348.

Kordeli, E., Davis, J., Trapp, B., and Bennett, V. (1990). An isoform of ankyrin is localized at nodes of Ranvier in myelinated axons of central and peripheral nerves. J. Cell Biol. *110*, 1341–1352.

Koticha, D., Maurel, P., Zanazzi, G., Kane-Goldsmith, N., Basak, S., Babiarz, J., Salzer, J., and Grumet, M. (2005). Neurofascin interactions play a critical role in clustering sodium channels, ankyrinG and βIV spectrin at peripheral nodes of Ranvier. Dev. Biol., in press.

Lacas-Gervais, S., Guo, J., Strenzke, N., Scarfone, E., Kolpe, M., Jahkel, M., De Camilli, P., Moser, T., Rasband, M.N., and Solimena, M. (2004). BetaIVSigma1 spectrin stabilizes the nodes of Ranvier and axon initial segments. J. Cell Biol. *166*, 983–990.

Lambert, S., Davis, J.Q., and Bennett, V. (1997). Morphogenesis of the node of Ranvier: co-clusters of ankyrin and ankyrin-binding integral proteins define early developmental intermediates. J. Neurosci. *17*, 7025–7036.

Lelianova, V.G., Davletov, B.A., Sterling, A., Rahman, M.A., Grishin,

E.V., Totty, N.F., and Ushkaryov, Y.A. (1997). Alpha-latrotoxin receptor, latrophilin, is a novel member of the secretin family of G protein-coupled receptors. J. Biol. Chem. *272*, 21504–21508.

Lemaillet, G., Walker, B., and Lambert, S. (2003). Identification of a conserved ankyrin-binding motif in the family of sodium channel alpha subunits. J. Biol. Chem. *278*, 27333–27339.

Loria, P.M., Hodgkin, J., and Hobert, O. (2004). A conserved postsynaptic transmembrane protein affecting neuromuscular signaling in Caenorhabditis elegans. J. Neurosci. *24*, 2191–2201.

Lustig, M., Zanazzi, G., Sakurai, T., Blanco, C., Levinson, S.R., Lambert, S., Grumet, M., and Salzer, J.L. (2001). Nr-CAM and neurofascin interactions regulate ankyrin G and sodium channel clustering at the node of Ranvier. Curr. Biol. *11*, 1864–1869.

Malhotra, J.D., Kazen-Gillespie, K., Hortsch, M., and Isom, L.L. (2000). Sodium channel beta subunits mediate homophilic cell adhesion and recruit ankyrin to points of cell-cell contact. J. Biol. Chem. *275*, 11383–11388.

Mathis, C., Denisenko-Nehrbass, N., Girault, J.A., and Borrelli, E. (2001). Essential role of oligodendrocytes in the formation and maintenance of central nervous system nodal regions. Development *128*, 4881–4890.

McEwen, D.P., and Isom, L.L. (2004). Heterophilic interactions of sodium channel beta 1 subunits with axonal and glial cell adhesion molecules. J. Biol. Chem. *279*, 52744–52752.

Melendez-Vasquez, C.V., Rios, J.C., Zanazzi, G., Lambert, S., Bretscher, A., and Salzer, J.L. (2001). Nodes of Ranvier form in association with ezrin-radixin-moesin (ERM)-positive Schwann cell processes. Proc. Natl. Acad. Sci. USA *98*, 1235–1240.

Melendez-Vasquez, C.V., Einheber, S., and Salzer, J.L. (2004). Rho kinase regulates schwann cell myelination and formation of associated axonal domains. J. Neurosci. *24*, 3953–3963.

Mohler, P.J., Gramolini, A.O., and Bennett, V. (2002). Ankyrins. J. Cell Sci. *115*, 1565–1566.

Myllyharju, J., and Kivirikko, K.I. (2004). Collagens, modifying enzymes and their mutations in humans, flies and worms. Trends Genet. *20*, 33–43.

Ohlmann, A., Goldwich, A., Flugel-Koch, C., Fuchs, A.V., Schwager, K., and Tamm, E.R. (2003). Secreted glycoprotein myocilin is a component of the myelin sheath in peripheral nerves. Glia *43*, 128–140.

Parkinson, N.J., Olsson, C.L., Hallows, J.L., McKee-Johnson, J., Keogh, B.P., Noben-Trauth, K., Kujawa, S.G., and Tempel, B.L. (2001). Mutant beta-spectrin 4 causes auditory and motor neuropathies in quivering mice. Nat. Genet. *29*, 61–65.

Peles, E., Nativ, M., Campbell, P.L., Sakurai, T., Martinez, R., Lev, S., Clary, D.O., Schilling, J., Barnea, G., Plowman, G.D., et al. (1995). The carbonic anhydrase domain of receptor tyrosine phosphatase beta is a functional ligand for the axonal cell recognition molecule contactin. Cell *82*, 251–260.

Peles, E., Nativ, M., Lustig, M., Grumet, M., Schilling, J., Martinez, R., Plowman, G.D., and Schlessinger, J. (1997). Identification of a novel contactin-associated transmembrane receptor with multiple domains implicated in protein-protein interactions. EMBO J. *16*, 978–988.

Poliak, S., and Peles, E. (2003). The local differentiation of myelinated axons at nodes of Ranvier. Nat. Rev. Neurosci. *4*, 968–980.

Poliak, S., Gollan, L., Martinez, R., Custer, A., Einheber, S., Salzer, J.L., Trimmer, J.S., Shrager, P., and Peles, E. (1999). Caspr2, a new member of the neurexin superfamily, is localized at the juxtaparanodes of myelinated axons and associates with K+ channels. Neuron *24*, 1037–1047.

Poliak, S., Matlis, S., Ullmer, C., Scherer, S.S., and Peles, E. (2002). Distinct claudins and associated PDZ proteins form different autotypic tight junctions in myelinating Schwann cells. J. Cell Biol. *159*, 361–372.

Poliak, S., Salomon, D., Elhanany, H., Sabanay, H., Kiernan, B., Pevny, L., Stewart, C.L., Xu, X., Chiu, S.-Y., Shrager, P., et al. (2003). Juxtaparanodal clustering of Shaker-like K^+ channels in myelinated axons depends on Caspr2 and TAG-1. J. Cell Biol. *162*, 1149–1160.

Raine, C.S. (1982). Differences between the nodes of Ranvier of large and small diameter fibres in the P.N.S. J. Neurocytol. *11*, 935–947.

Raine, C.S. (1984). On the association between perinodal astrocytic processes and the node of Ranvier in the C.N.S. J. Neurocytol. *13*, 21–27.

Ratcliffe, C.F., Westenbroek, R.E., Curtis, R., and Catterall, W.A. (2001). Sodium channel beta1 and beta3 subunits associate with neurofascin through their extracellular immunoglobulin-like domain. J. Cell Biol. *154*, 427–434.

Saito, F., Moore, S.A., Barresi, R., Henry, M.D., Messing, A., Ross-Barta, S.E., Cohn, R.D., Williamson, R.A., Sluka, K.A., Sherman, D.L., et al. (2003). Unique role of dystroglycan in peripheral nerve myelination, nodal structure, and sodium channel stabilization. Neuron *38*, 747–758.

Salzer, J.L. (2003). Polarized domains of myelinated axons. Neuron *40*, 297–318.

Schafer, D.P., Bansal, R., Hedstrom, K.L., Pfeiffer, S.E., and Rasband, M.N. (2004). Does paranode formation and maintenance require partitioning of neurofascin 155 into lipid rafts? J. Neurosci. *24*, 3176–3185.

Scherer, S.S., Xu, T., Crino, P., Arroyo, E.J., and Gutmann, D.H. (2001). Ezrin, radixin, and moesin are components of Schwann cell microvilli. J. Neurosci. Res. *65*, 150–164.

Spiegel, I., Salomon, D., Erne, B., Schaeren-Wiemers, N., and Peles, E. (2002). Caspr3 and caspr4, two novel members of the caspr family are expressed in the nervous system and interact with PDZ domains. Mol. Cell. Neurosci. *20*, 283–297.

Stone, E.M., Fingert, J.H., Alward, W.L., Nguyen, T.D., Polansky, J.R., Sunden, S.L., Nishimura, D., Clark, A.F., Nystuen, A., Nichols, B.E., et al. (1997). Identification of a gene that causes primary open angle glaucoma. Science *275*, 668–670.

Tait, S., Gunn-Moore, F., Collinson, J.M., Huang, J., Lubetzki, C., Pedraza, L., Sherman, D.L., Colman, D.R., and Brophy, P.J. (2000). An oligodendrocyte cell adhesion molecule at the site of assembly of the paranodal axo-glial junction. J. Cell Biol. *150*, 657–666.

Tao-Cheng, J.H., and Rosenbluth, J. (1983). Axolemmal differentiation in myelinated fibers of rat peripheral nerves. Brain Res. *285*, 251–263.

Tsuda, H., Sasai, N., Matsuo-Takasaki, M., Sakuragi, M., Murakami, Y., and Sasai, Y. (2002). Dorsalization of the neural tube by Xenopus tiarin, a novel patterning factor secreted by the flanking nonneural head ectoderm. Neuron *33*, 515–528.

Vabnick, I., Novakovic, S.D., Levinson, S.R., Schachner, M., and Shrager, P. (1996). The clustering of axonal sodium channels during development of the peripheral nervous system. J. Neurosci. *16*, 4914–4922.

Vabnick, I., Messing, A., Chiu, S.Y., Levinson, S.R., Schachner, M., Roder, J., Li, C., Novakovic, S., and Shrager, P. (1997). Sodium channel distribution in axons of hypomyelinated and MAG null mutant mice. J. Neurosci. Res. *50*, 321–336.

Waxman, S.G., and Ritchie, J.M. (1993). Molecular dissection of the myelinated axon. Ann. Neurol. *33*, 121–136.

Yang, Y., Lacas-Gervais, S., Morest, D.K., Solimena, M., and Rasband, M.N. (2004). BetaIV spectrins are essential for membrane stability and the molecular organization of nodes of Ranvier. J. Neurosci. *24*, 7230–7240.

Yokoe, H., and Anholt, R.R. (1993). Molecular cloning of olfactomedin, an extracellular matrix protein specific to olfactory neuroepithelium. Proc. Natl. Acad. Sci. USA *90*, 4655–4659.